

# High-power continuous-wave mid-infrared radiation generated by difference frequency mixing of diode-laser-seeded fiber amplifiers and its application to dual-beam spectroscopy

D. G. Lancaster, D. Richter, R. F. Curl, and F. K. Tittel

*Rice Quantum Institute, Rice University, Houston, Texas 77005*

L. Goldberg and J. Koplou

*Optical Sciences Division, Naval Research Laboratory, Washington, D.C. 20375-5672*

Received August 2, 1999

We report the generation of up to 0.7 mW of narrow-linewidth ( $<60$ -MHz) radiation at  $3.3\ \mu\text{m}$  by difference frequency mixing of a Nd:YAG-seeded 1.6-W Yb fiber amplifier and a 1.5- $\mu\text{m}$  diode-laser-seeded 0.6-W Er/Yb fiber amplifier in periodically poled LiNbO<sub>3</sub>. A conversion efficiency of 0.09%/W ( $0.47\ \text{mW W}^{-2}\ \text{cm}^{-1}$ ) was achieved. A room-air CH<sub>4</sub> spectrum acquired with a compact 80-m multipass cell and a dual-beam spectroscopic configuration indicates an absorption sensitivity of  $\pm 2.8 \times 10^{-5}$  ( $\pm 1\sigma$ ), corresponding to a sub-parts-in-10<sup>9</sup> (ppb) CH<sub>4</sub> sensitivity (0.8 ppb). © 1999 Optical Society of America

OCIS codes: 280.3420, 300.6340, 190.2620, 060.2320.

Milliwatt-level sources of stable single-frequency radiation in the 3–5- $\mu\text{m}$  spectral region are required for applications such as high-resolution molecular spectroscopy, trace-gas detection, and pollution monitoring. The availability of increased mid-IR power in such applications will allow more-sensitive and -rapid spectroscopic measurements, owing to an increased signal-to-noise ratio, the possibility of longer optical path lengths, and the use of enhanced detection techniques. Narrow-band mid-IR sources that operate at room temperature and powers in excess of  $\sim 200\ \mu\text{W}$  are required for long-term, sensitive, and continuous monitoring of key atmospheric trace-gas species. Difference frequency generation (DFG) of near-IR laser sources is a convenient technique to produce tunable mid-IR radiation, although typically the DFG conversion efficiency is low. For mid-IR generation cryogenically cooled Pb salt diode lasers have been routinely used,<sup>1</sup> and more recently quantum cascade lasers were used.<sup>2</sup> Continuous-wave singly resonant optical parametric oscillators have been demonstrated,<sup>3</sup> although their repetitive wavelength scanning ability across molecular lines (at hertz to kilohertz rates) and robustness for high-resolution molecular spectroscopy have not yet been demonstrated to our knowledge.

For DFG-based mid-IR sources in the 3–5- $\mu\text{m}$  region, periodically poled lithium niobate (PPLN) is the nonlinear material of choice. DFG mixing of a Ti:sapphire–Nd:YAG system generated up to 500  $\mu\text{W}$  of power,<sup>4</sup> and a diode-seeded semiconductor amplifier system generated 31  $\mu\text{W}$  of power.<sup>5</sup> Conversion efficiency in PPLN can be enhanced by addition of a channel waveguide with reported conversion efficiencies of up to 105%/W (Ref. 6); however, to our knowledge high-power capability has not been demonstrated, as only 250 nW of power at 2.8  $\mu\text{m}$  has been generated to date. To improve the ruggedness of DFG for field applications and reduce alignment requirements we have developed sensors that use pump-beam fiber delivery and

a fiber wavelength-division multiplexer for pump-beam combination into a single fiber. These sensors include an 11- $\mu\text{W}$  DFG system in which the pump beams were amplified by an in-line diode-pumped Yb amplifier and a passive Er/Yb codoped fiber amplifier.<sup>7</sup> A portable widely tunable sensor (3.3–4.3  $\mu\text{m}$ ) based on a diode-seeded Yb amplifier and an 8.14–870-nm external-cavity diode-laser system that produces  $\sim 3\ \mu\text{W}$  was described in Ref. 8.

In this Letter we report a potentially compact and efficient all-solid-state system with fiber-optic coupling that generates up to 0.7 mW of mid-IR power in a diffraction-limited beam. The measured bandwidth is  $<60$  MHz, and we have demonstrated sensitive dual-beam spectroscopy of CH<sub>4</sub> in an 80-m Herriot cell.

A schematic of the DFG experimental configuration is shown in Fig. 1. The mid-IR source is based on low-power laser sources at 1 and 1.5  $\mu\text{m}$ , which seed 1.5-W Yb and 0.6-W Er/Yb fiber amplifiers, respectively. One seed source for this experiment was a cw 1.064- $\mu\text{m}$  Nd:YAG laser that was used to simulate a diode laser emitting near this wavelength (e.g., a 1083-nm distributed Bragg reflector diode laser). We coupled 20 mW of its output into a single-mode fiber to seed the Yb amplifier after it passed through a  $-45$ -dB optoisolator. The backward-propagating light from the 1064-nm Yb amplifier was monitored for evidence of power instabilities owing to stimulated Brillouin scattering (SBS) and Rayleigh scattering. This was accomplished by use of a fused-silica wedge placed at 45° in the beam path, which directed 9% of the light to a Si photodiode ( $\sim 50$  ns). A 2-mW fiber pigtailed 1.560- $\mu\text{m}$  distributed-feedback telecommunication diode laser with  $-80$  dB of in-line optical isolation was used as the second seed source. To minimize backreflections to the high-gain amplifiers and prevent formation of optical etalons, we ensured that all optical fiber terminations that were used in the sensor were terminated with connectors that had their ends

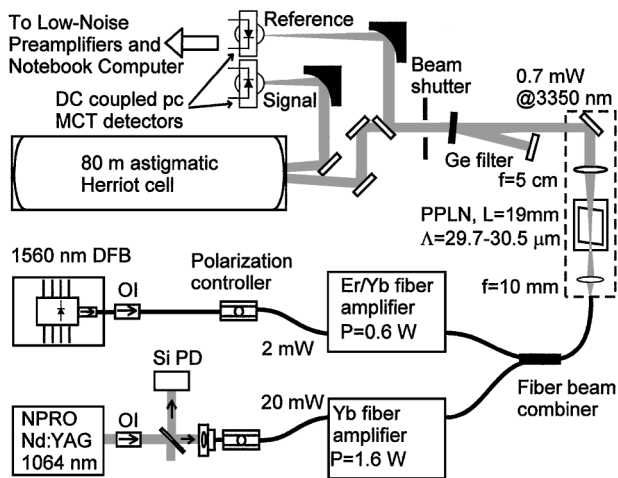


Fig. 1. Schematic of the experimental DFG configuration: DFB, distributed feedback; OI's, optoisolators; PD, photodiode; NPRO, nonplanar ring oscillator.

polished at  $8^\circ$  off normal incidence. We placed in-line polarization controllers on each input fiber to set the linear vertical polarization states required for quasi-phase matching.

The rare-earth amplifiers are based on doped double-clad fibers that are pumped by single 975-nm 4-W diode lasers coupled into the outer hexagonal cross-section cladding by a V-groove configuration.<sup>9</sup> The output from each fiber amplifier was combined into a single fiber by use of a fiber wavelength-division multiplexer. The fiber output was then imaged by an  $f = 10$  mm antireflection-coated achromat lens configured for a magnification of  $11\times$  into a 19-mm-long PPLN crystal, resulting in estimated beam spot diameters of the 1.06- and 1.56- $\mu\text{m}$  beams of 63 and 89  $\mu\text{m}$ , respectively. The PPLN crystal, which contained nine quasi-phase-matched channels with periods ranging from 29.7 to 30.5  $\mu\text{m}$  in 0.1- $\mu\text{m}$  increments, was mounted on a Peltier element for temperature control and antireflection coated for the pump, signal, and idler wavelengths. The DFG beam was collimated by an  $f = 5$  cm CaF<sub>2</sub> plano-convex lens and the residual pump light removed by an antireflection-coated Ge filter.

We used a calibrated thermopile detector to alternately measure the incident pump and DFG powers. A reference beam for dual-beam spectroscopic measurements was provided by the front surface's 29% reflection from an uncoated ZnSe wedge placed in the beam at  $45^\circ$ . The reference beam was then directed to an off-axis  $f = 3$  cm parabolic mirror, where the radiation was focused onto the HgCdTe (MCT) reference detector. The remaining radiation was directed through an astigmatic Herriot cell configured for a path length of 80 m before being directed onto a second MCT detector (data channel). The MCT detectors were operated in a photoconductive mode and dc coupled to preamplifiers with 3-dB bandwidths of 200 kHz. Each detector had an area of 1 mm<sup>2</sup> and was operated at a temperature of  $-65^\circ\text{C}$  by use of integrated three-stage Peltier cooling elements.

The data for spectroscopic measurements were recorded by two separate 16-bit analog-digital cards sampling in parallel at 100 kHz and interfaced to a laptop Pentium II PC running Labview (National Instruments) and Windows98. A beam shutter after the Ge filter allowed the dark voltage of each detector to be measured. We normalized the acquired data to transmission by taking the natural logarithm of the ratio of each detector voltage less the detector dark voltage. Any nonlinearity between the detectors or residual low-frequency optical fringes were removed by subtraction of a polynomial function fitted to the spectrum baseline. We then obtained a normalized transmission spectrum by taking the exponential.

In Fig. 2, a conversion efficiency of  $0.89\ \text{mW W}^{-2}$  ( $0.47\ \text{mW W}^{-2}/\text{cm}^{-1}$ ) is shown with a maximum power of 0.7 mW generated for the 19-mm-long PPLN crystal. Our measured slope efficiency compares reasonably with the theoretically expected conversion efficiency of  $0.76\ \text{mW W}^{-2}/\text{cm}^{-1}$ .<sup>10</sup> The plotted powers were corrected for losses from optical surfaces (uncorrected power, 0.55 mW). Phase matching was obtained with the 30.1- $\mu\text{m}$  grating period at a temperature of  $45^\circ\text{C}$ . To measure the time-averaged linewidth of the DFG radiation we recorded the Doppler-broadened spectrum of 0.4 Torr of CH<sub>4</sub> in a 3-cm-long cell, as shown in Fig. 3 (Doppler-broadened FWHM of CH<sub>4</sub> is 276 MHz). This measurement was taken over 100 averages at a 0.1-kHz scan rate. The Doppler linewidth of CH<sub>4</sub> was then deconvolved from the acquired spectra to give a DFG linewidth measurement of  $<60$  MHz (assumed to be Gaussian).

A spectrum of room air acquired over a  $0.8\text{-cm}^{-1}$  scan range is shown in Fig. 4, which covers two H<sub>2</sub>O lines and the <sup>12</sup>CH<sub>4</sub>  $P(3)\ \nu_3$  rovibrational lines. This spectrum was taken at a reduced pressure of 88 Torr in an 80-m path-length Herriot cell. We calculated a molecular concentration of  $2021 \pm 21$  parts in  $10^9$  (ppb)

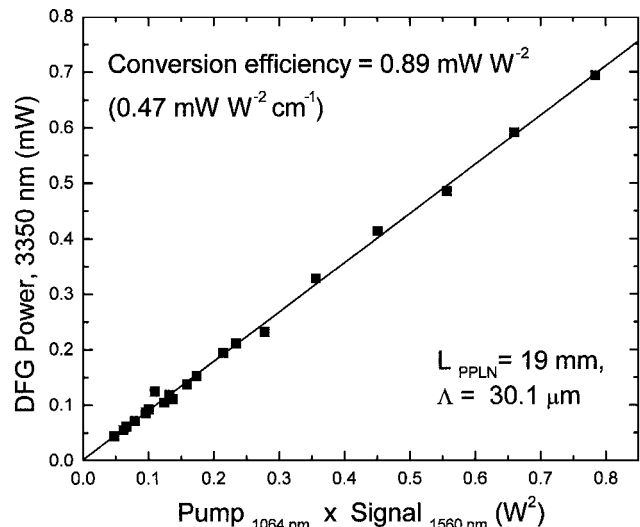


Fig. 2. Measured conversion efficiency of  $0.89\ \text{mW W}^{-2}$  ( $0.47\ \text{mW W}^{-2}/\text{cm}^{-1}$ ) for a 19-mm-long PPLN crystal pumped by two fiber-amplified channels at 1064 and 1560 nm.

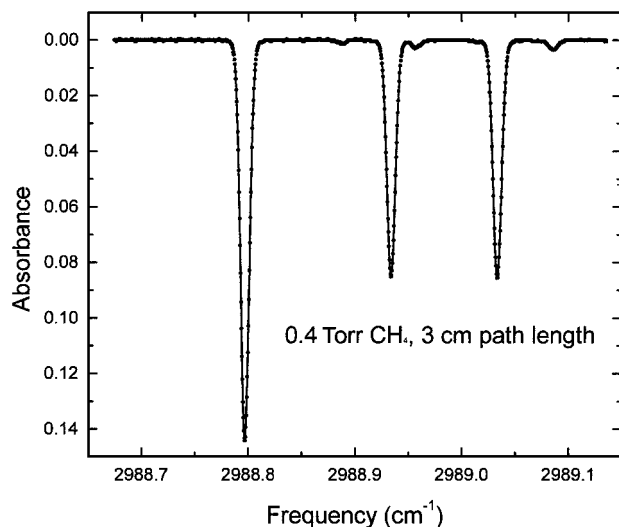


Fig. 3. Doppler-broadened spectra of 0.4 Torr of  $\text{CH}_4$  in a 3-cm cell. This measurement was taken over 100 averages at a 0.1-kHz wavelength scan rate and demonstrates a sensor linewidth of  $<60$  MHz.

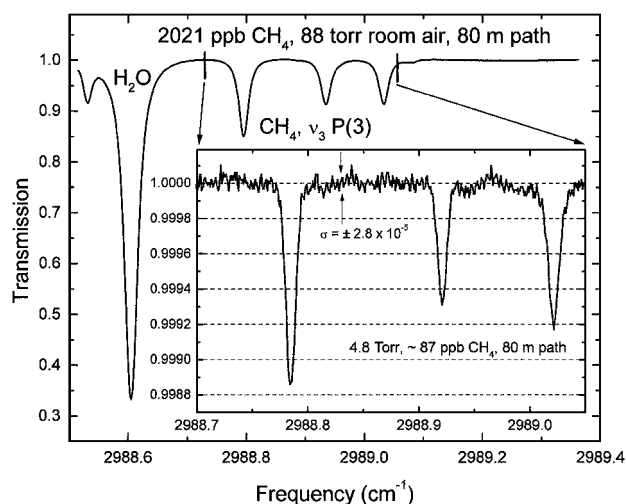


Fig. 4. Room-air spectrum of the  $\text{CH}_4 P(3) \nu_3$  rovibrational lines at  $P = 88$  Torr and two  $\text{H}_2\text{O}$  lines. The inset is a low-pressure  $\text{CH}_4$  spectrum in the same spectral region ( $\sim 87$  ppb of  $\text{CH}_4$  in nitrogen).

$\text{CH}_4$  in air by fitting a Voigt line shape to each  $\text{CH}_4$  peak and compared the resulting integrated line-shape areas with those obtained from a cylinder of calibrated air containing 1772.7-ppb  $\text{CH}_4$ . The  $\pm 21$  ppb error is attributable to the difficulty in estimating the background value for each  $\text{CH}_4$  absorption line fitted, due to the overlap of the five primary absorption peaks and three weaker peaks. The inset of Fig. 4 shows a reduced-frequency range spectrum of a low  $\text{CH}_4$  concentration ( $\sim 87$  ppb) in nitrogen at a cell pressure of 4.8 Torr and is an average of 1000 spectra (10-s average and 200-Hz detection bandwidth). This spectrum was acquired to display the  $P(3)$  rovibrational lines and baseline noise on the same scale as well as to reduce the

effect of pressure broadening on the line shapes. The baseline noise has a  $\pm 1\sigma$  magnitude of  $\pm 2.8 \times 10^{-5}$ , which we attribute to detector–preamplifier  $1/f$  noise, thereby implying a normalized detection sensitivity of  $4.0 \times 10^{-6} \text{ Hz}^{-1/2}$  and an estimated  $\text{CH}_4$  detection sensitivity of 4.3 ppb m  $\text{Hz}^{-1/2}$ .

During initial characterization of the sensor, a spiking behavior in the 1- $\mu\text{m}$  pump power was observed. We attributed this behavior to a combination of SBS and Rayleigh scattering occurring in the pump-beam delivery fiber, which produced backward-propagating pulses that were subsequently amplified in the high-gain Yb amplifier, thereby leading to power instability. To eliminate the SBS effects in the fiber we shortened the delivery fiber from 7 to 1.5 m, which increased the calculated threshold for SBS from 1.6 to 7.3 W, assuming a 5.7- $\mu\text{m}$  field diameter in the fiber.<sup>11</sup> Future work will focus on the use of dual-beam wavelength modulation spectroscopy<sup>12</sup> to improve sensitivity and sensor optimization to permit long-term monitoring of low-concentration gases such as  $\text{CH}_4$  and  $\text{H}_2\text{CO}$ .

In summary, DFG radiation of up to 0.7 mW at 3.3  $\mu\text{m}$  is reported with a measured bandwidth of  $<60$  MHz. A minimum absorption of  $\pm 2.8 \times 10^{-5}$  with dual-beam absorption spectroscopy was achieved. This work demonstrates a significant increase in both power and sensitivity over previously reported DFG-based spectroscopic sources and thereby will open up new gas detection applications.

This research was supported by NASA, the Texas Advanced Technology Program, the Welch Foundation, the National Science Foundation, and the U.S. Office of Naval Research. T. K. Tittel's e-mail address is tkt@rice.edu.

## References

1. A. Fried, S. Sewell, B. Henry, B. P. Wert, and T. Gilpin, *J. Geophys. Res.* **102**, 6253 (1997).
2. F. Capasso, C. Gmachl, D. L. Sivco, and A. Y. Cho, *Phys. World* **12**, 27 (1999).
3. M. E. Klein, D. H. Lee, J. P. Meyn, K. J. Boller, and R. Wallenstein, *Opt. Lett.* **24**, 1142 (1999).
4. L. Goldberg, W. K. Burns, and R. W. McElhanon, *Opt. Lett.* **20**, 1280 (1995).
5. A. Balakrishnan, S. Sanders, S. DeMars, J. Webjorn, D. W. Nam, R. J. Lang, D. G. Mehuys, R. G. Waarts, and D. F. Welch, *Opt. Lett.* **21**, 952 (1996).
6. D. Hofmann, G. Schreiber, C. Haase, H. Herrmann, W. Grundkötter, R. Ricken, and W. Sohler, *Opt. Lett.* **24**, 896 (1999).
7. L. Goldberg, J. Koplow, D. G. Lancaster, R. F. Curl, and F. K. Tittel, *Opt. Lett.* **23**, 1517 (1998).
8. D. G. Lancaster, D. Richter, and F. K. Tittel, "Portable fiber coupled diode laser based sensor for multiple trace gas detection," *Appl. Phys. B* (to be published).
9. L. Goldberg, J. Koplow, and D. A. V. Kliner, *Opt. Lett.* **24**, 673 (1999).
10. P. Canarelli, Z. Benko, R. F. Curl, and F. K. Tittel, *J. Opt. Soc. Am. B* **9**, 197 (1992).
11. G. P. Agrawal, *Nonlinear Fiber Optics* (Academic, San Francisco, Calif., 1989).
12. P. Werle, *Spectrochim. Acta A* **54**, 197 (1998).